Air-Gapped Current Transformer simulation and accuracy assessment

Luis Felipe Ceron Oliver
Department of Engineering
Durham University
Durham, United Kingdom
luis.f.ceron-oliver@durham.ac.uk

Qing Wang
Department of Engineering
Durham University
Durham, United Kingdom
qing.wang@durham.ac.uk

Dagou Zeze
Department of Engineering
Durham University
Durham, United Kingdom
d.a.zeze@durham.ac.uk

***Abstract*—The implementation of smart grids makes it necessary to have reliable and efficient measuring devices. Current sensors used for metering purposes in the grid must be accurate enough to overcome new challenges that power networks face such as injection of undesirable Direct Current (DC) in the system. A Current Transformer (CT) is a transformer widely used to measure current in an electrical circuit. This paper describes the modelling and simulation of a CT with a variable air gap, provides different results of cases with different air gap ratios and evaluates the respective primary and secondary currents in each case according to the standard IEC for instrument transformers. Results show that if an air gap is present, the transformer only reached an accuracy class of 0.5 when the air gap ratio is 0.001.**

Keywords—Current Transformer, Air-Gapped CT, Jiles-Atherton, DC injection.

I. Introduction

A CT is an elemental device in power networks, providing a way to isolate a current in the system either for protection or for measuring purposes in the grid. The main function of CTs is to deliver an accurate representation when a primary current is introduced, however this is not always possible. That is why the behaviour of CTs in power networks has been studied for several years, with a special interest in the saturation of CTs due to their magnetic properties. CT saturation may lead to an inaccurate representation of the primary current, which could include amplitude error and phase error. Both will cause incorrect operation of protection devices or measuring equipment.

In the past few years, the implementation of smart grids has added an extra challenge to current sensors such as CTs. Smart grids integrate a diverse quantity of sources and devices which may inject an undesirable distortion into the network. Special attention should be paid to address the DC that is introduced to the grid by power electronic devices. This undesirable DC may cause a loss of accuracy in smart meters, which are used by power companies to monitor the current consumed by the user.

Designers of CTs endeavour to decrease transformation errors in CTs because these will have an impact in measurement systems [1]. For instance, if the accuracy of the CT decreases, the measurement of the total consumption in a smart meter will be erroneous. Hence, taking into consideration that smart meters are used for revenue purposes, an incorrect bill will be charged to the user, which can affect both consumers and energy suppliers.

A disproportionate injection of DC may cause transformer saturation, transformer magnetizing current distortion and malfunction of protective equipment [2]. Ripka [3] obtained that a low-cost CT has an error of 10 to 40% in current and power measurement in the existence of a 50 A DC. Similar results were obtained for a high-performance CT with a core constructed of a nanocrystalline material.

According to Bachinger et al. [4] with a high level of DC, the excitation current increases dramatically and suffers distortions. Moreover, the use of DC in testing CT circuits may also cause remanence. Depending on the type of steel, a remanent flux may exist as high as 90% of the total saturation flux, that is 90% of the total magnetic flux when the CT is considered to be under saturation [5].

CT saturation due to injection of DC has been treated using different approaches. One of the most common approaches is to compensate the CT through a feedback loop [2, 3]. However, this requires the use of active components that could undermine the stability of the measuring systems [3].

Another solution for the last problem is to add an air gap in the core of the CT. Air-Gapped Current Transformers (AGCT) have been used to deal with the remanent flux that causes saturation of the transformer in systems for protection purposes [6]. Some studies have been conducted about AGCTs, however these have been focused on the performance of AGCTs in protection schemes, not in metering applications.

The purpose of the paper is to demonstrate the main characteristics and performance that the AGCTs have in power measurement through the use of simulations. It is expected to observe the loss of accuracy that the different lengths of air gaps may cause in the output of the CT. Additionally, results obtained are evaluated according to an international standard for instrument transformers.

II. Theory of the CT and AGCT

A. Current Transformer basics

Current transformers are sensors used to measure current in electrical networks, either for metering or for protection purposes [7]. To achieve the mentioned purposes, it is necessary to decrease the current of the power network so it can be easily managed [8]. A CT can be seen as two sets of wire windings around an iron core, and its operation is based on the electromagnetic induction principle [9]. Fig. 1 shows the physical representation of a CT, where I_P is the primary current, H is the magnetic field strength, ϕ is the magnetic flux, V_S is the secondary voltage and I_S refers to the secondary current.

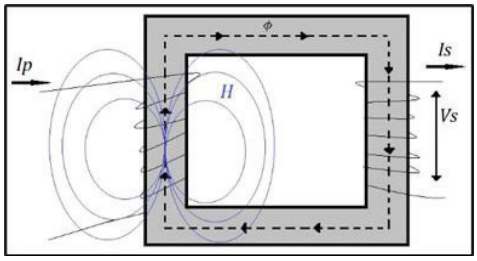

Fig. 1 CT representation.

Fig. 2 shows the equivalent electrical circuit of the CT. The excitation current I_E is observed, which is the current necessary to magnetize the core of the CT [7]. L_m refers to the excitation inductance, and R_S and L_S are the total resistance and inductance of the secondary, respectively [10].

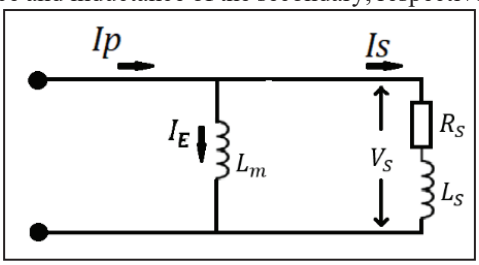

Fig. 2. CT equivalent circuit.

From Fig. 2, the basic equations of the CT can be obtained [10].

$$I_S R_S + L_S \frac{dI_S}{dt} = N_S A \frac{dB}{dt} \tag{1}$$

$$I_P = I_E + I_S \tag{2}$$

$$N_S A \frac{dB}{dt} + L_S \frac{dI_E}{dt} + I_E R_S = I_P R_S + L_S \frac{dI_P}{dt} \tag{3}$$

In (1) and (3), N_S is the number of turns in the secondary winding, A is the core cross section area and B is the magnetic flux density in the core.

B. Air-Gapped Current Transformer

Current in a CT may reach 10 or one hundred times the current for which they are designed (rated current) when short-circuit incidents occur, which causes saturation of the core. This will produce errors and malfunction of protection or measuring equipment. Hence, in order to solve the issue, manufacturers inserted a small air gap in the core of the CT [10], as can be seen in Fig. 3. Adding air gaps in the magnetic circuit of a core reduces the remanent flux. This flux can be decreased to a low value, such as 10% of the total saturation flux [11].

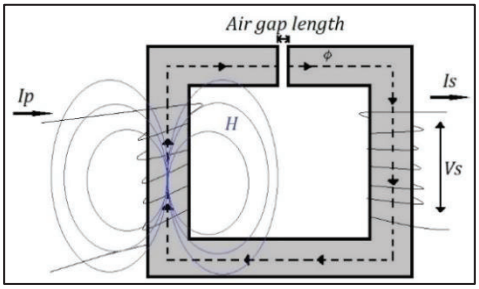

Fig. 3. Air-Gapped CT representation.

III. Modelling of the AGCT

A. Jiles-Atherton model

The modelling and simulation of an AGCT are necessary to understand the behaviour of these sensors and to be able to predict and compare the obtained results when the AGCT can be built. Then, for the future needs of the research, the simulation of the AGCT is fundamental and a model was developed based on Jiles-Atherton (J-A) theory [12]. The model was implemented in MATLAB-Simulink.

Jiles-Atherton theory is commonly used to model the non-linear behaviour of magnetic materials [13]. It makes possible the use of a series of mathematical expressions that provide the BH hysteresis curve through five parameters that depend on the material characteristics [12, 14, 15] and therefore it is possible to simulate the performance of a CT core. The five Jiles-Atherton parameters are:

- M_s: saturation magnetic moment of the core material.
- a: shape of the anhysteric magnetization curve.
- c: domain flexing parameter.
- k: energy loss coefficient.
- α: interdomain coupling factor.

The most important feature of the J-A theory of ferromagnetic hysteresis is the fragmentation of the magnetization M into its reversible (M_{rev}) and irreversible (M_{irr}) components. Equation (4) describes this fragmentation.

$$M = M_{irr} + M_{rev} \tag{4}$$

The effective field H_e and the magnetic flux density B are calculated by (5) and (6).

$$H_e = H + \alpha M \tag{5}$$

$$B = \mu_0 (H + M) \tag{6}$$

where μ_0 is the permeability of free space.

The Langevin function is used to describe the anhysteric magnetization M_{an} in (7).

$$M_{an} = M_s \left(coth \frac{H_e}{a} - \frac{a}{H_e} \right) \tag{7}$$

Then, the irreversible susceptibility can be defined by the next hysteresis differential equation:

$$\frac{dM_{irr}}{dH} = \frac{M_{an} - M_{irr}}{\frac{\delta k}{\mu_0} - \alpha (M_{an} - M_{irr})} \tag{8}$$

where δ corresponds to the sign of $\frac{dH}{dt}$, a directional parameter which takes a value of +1 when $\frac{dH}{dt} > 0$ and -1 when $\frac{dH}{dt} < 0$.

The reversible magnetization decreases the difference between the irreversible magnetization and the anhysteric magnetization in a specific field strength. This relationship is described in (9).

$$M_{rev} = c\,(M_{an} - M_{irr}) \tag{9}$$

After that, the hysteresis differential equation for reversible susceptibility can be established:

$$\frac{dM_{rev}}{dH} = c \left(\frac{dM_{an}}{dH} - \frac{dM_{irr}}{dH} \right) \tag{10}$$

Finally, combining (4) to (10), the resultant hysteresis differential equation for magnetization M can be obtained by adding together the results of the irreversible and the reversible magnetization:

$$\frac{dM}{dH} = \frac{dM_{rev}}{dH} + \frac{dM_{irr}}{dH} \tag{11}$$

$$\frac{dM}{dH} = \frac{1}{(1+c)} \frac{(M_{an} - M)}{\frac{\delta k}{\mu_0} - \alpha(M_{an} - M)} + \frac{c}{(1+c)} \frac{dM_{an}}{dH} \tag{12}$$

However, (12) contains derivatives with respect to H, meaning that it has to be reformulated so that the derivatives are with respect to time. To accomplish this, both sides of (12) are multiplied by $\frac{dH}{dt}$ [13]. Equation (13) shows the final relationship of J-A parameters, magnetization M and magnetic field H.

$$\frac{dM}{dt} = \frac{1}{(1+c)} \frac{dH}{dt} \frac{(M_{an} - M)}{\frac{\delta k}{\mu_0} - \alpha(M_{an} - M)} + \frac{c}{(1+c)} \frac{dM_{an}}{dt} \tag{13}$$

B. Air-Gap Current Transformer model

With the purpose of simulating the behaviour of an AGCT, it is necessary to insert some formulae. Equations (14) to (17) are obtained from the work developed by Muthumuni et al. [16].

$$V_S = I_S R_S + L_S \frac{d}{dt} I_S + I_S R_B + L_B \frac{d}{dt} I_S \tag{14}$$

$$V_S = K_{Siron} \frac{d}{dt} (N_P I_P - N_S I_S) \tag{15}$$

$$K_{Siron} = \frac{N_S A_{iron} \mu_0 (1 + S_{iron})}{\left(l_{iron} + \left(\frac{A_{iron}}{A_{air}} \right) l_{air} (1 + S_{iron}) \right)} \tag{16}$$

$$S_{iron} = \frac{l_{iron}}{\mu_{iron} A_{iron}} \tag{17}$$

where K_{Siron} is the constant of reluctance of the iron path, S_{iron} is the reluctance of the iron path, A_{iron} corresponds to the iron core area, A_{air} is the air gap area, l_{iron} is the iron core length, l_{air} is the air gap length and μ_{iron} refers to the permeability of iron.

Equation (14) is obtained from the equivalent circuit of the CT while (15) comes from the relationship between the secondary voltage and the magnetic flux density. With both equations mentioned before a differential formula is obtained in which the only unknown parameter is I_S:

$$\frac{d}{dt} I_S (L_S + L_B + K_{Siron} N_S) + I_S (R_S + R_B) - K_{Siron} N_P \frac{d}{dt} I_P = 0$$

C. Model constructed on Simulink

Using the equations presented above, the model was implemented in MATLAB-Simulink. The equations allow us to obtain the respective BH curve of the AGCT using the Jiles-Atherton parameters for the respective material.

Highlighted blue blocks in Figs. 4 and 5 represent the input values in the system such as the J-A parameters, permeability of the material, resistances, inductances, etc. The main subsystem shown in Fig. 4 is used to calculate the magnetic flux density B of the system and the outcome is the BH curve. The subsystem indicated by the arrow in Fig. 4 calculates the anhysteric magnetization M_{an}.

The subsystem shown in Fig. 5 is used to analyse the behaviour of the AGCT considering parameters such as length, area of the core, permeability of the material, windings and primary current. This subsystem is used to calculate the total magnetic field H and the secondary current I_S. The output of the system is the comparison between $N_P I_P$ and $N_S I_S$ which represents the error of the AGCT.

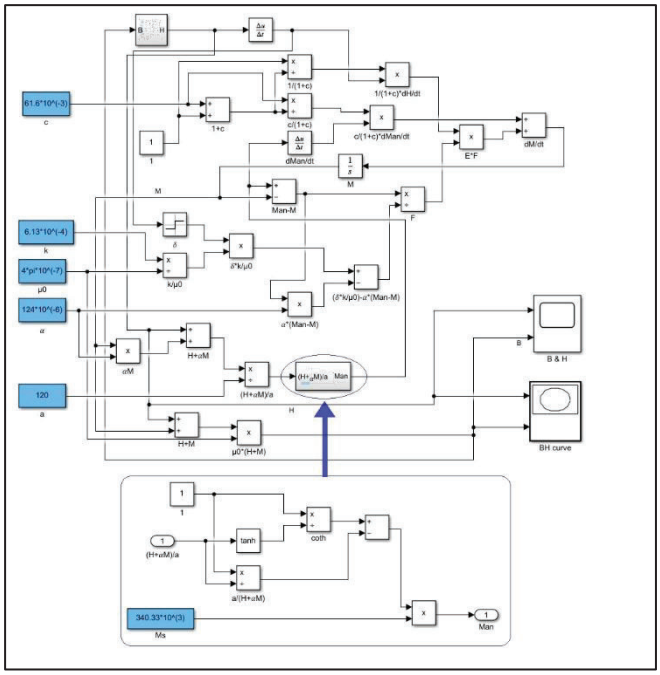

Fig. 4. Subsystem used for calculating magnetization and magnetic flux density.

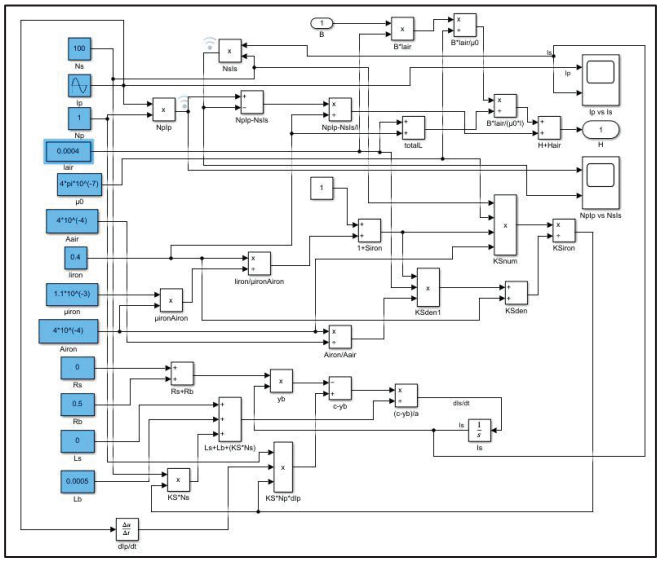

Fig. 5. Subsystem used to obtain magnetic field of the AGCT and secondary current.

In this case, the current simulation was carried out using the values of a non-oriented Fe-3.2 wt%Si [17, 18]. The values are: a =120 A/m, c =0.0616, k =488 A/m, M_s=340.33x10^3 A/m, α=124x10^{-6}. Fig. 6 shows the obtained BH curve of the material.

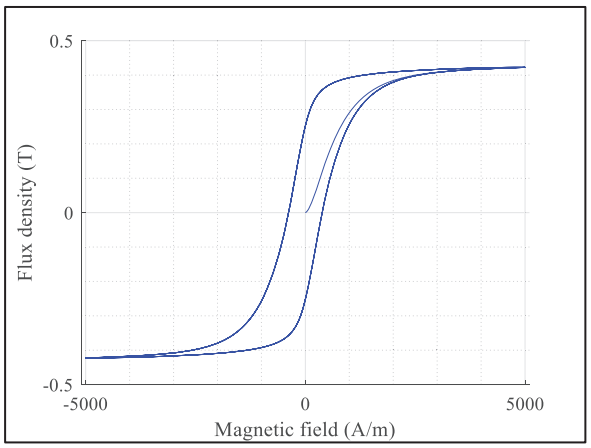

Fig. 6. BH curve of the non-oriented Fe-3.2 wt%Si.

The simulations were carried out to analyse the accuracy of the CT under different air gap ratios. The air gap ratios used for the simulation are 0.001, 0.002, 0.003, 0.004 and 0.005. This means that the air gap length corresponds to 0.001% of the total length of the magnetic core. Additionally, a case with no air gap was simulated. The primary currents used were 100 A and 200 A, and the different air gap ratio values were tested for each primary current. The values used for the simulation of the AGCT were N_P=1, N_S=100, R_S=0 Ω, L_S=0 H, R_B=0.5 Ω, L_B=0.5 mH, A_{air}=A_{iron}=4x10^{-4} m^2, l_{iron}=0.4 m and μ_{iron}=1.1x10^{-3} H/m.

IV. Results

Figs. 7 and 8 show the resultant comparison between N_PI_P and N_SI_S under for three different lengths of air gap under a primary current of 100 A and 200 A respectively.

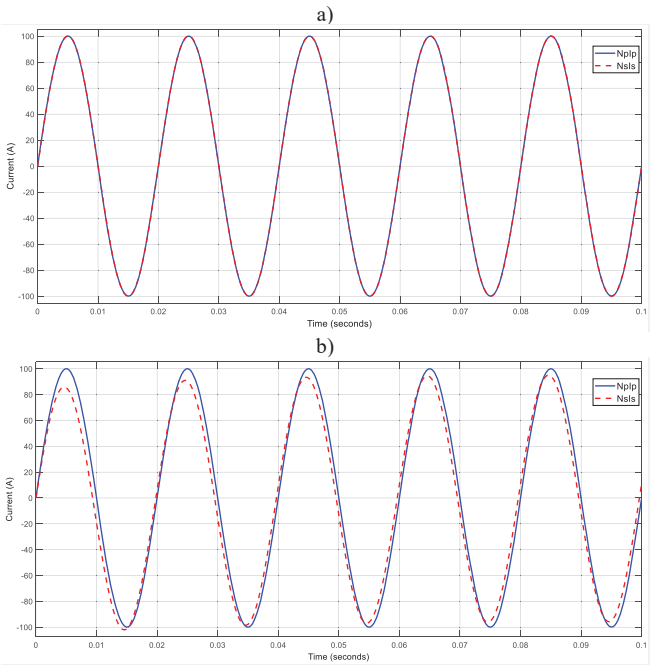

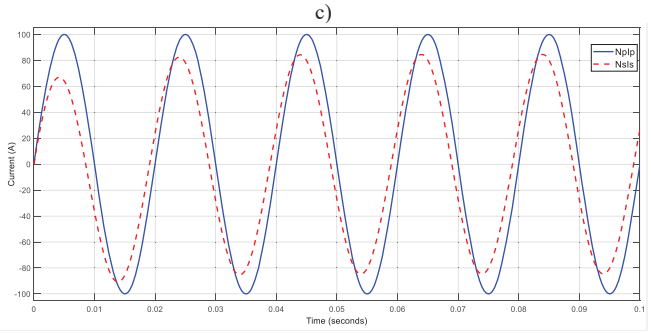

Fig. 7. Comparison between primary and proportional secondary current with a primary current of 100 A at a) Air gap ratio=0, b) Air gap ratio=0.001 and c) Air gap ratio=0.003.

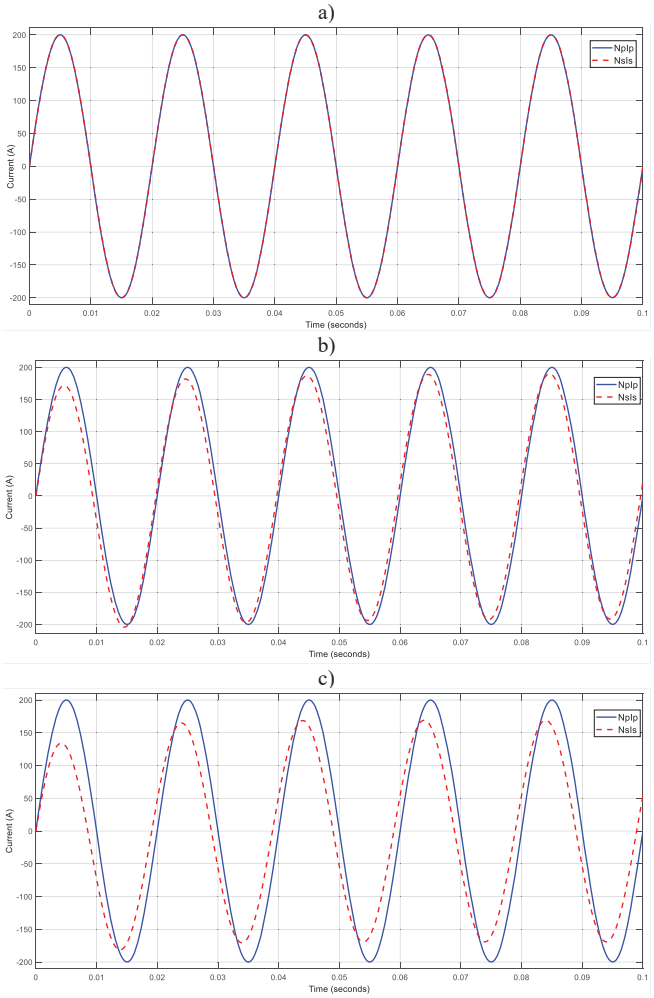

Fig. 8. Comparison between primary and proportional secondary current with a primary current of 200 A at a) Air gap ratio=0, b) Air gap ratio=0.001 and c) Air gap ratio=0.003.

The error ratio and phase displacement values for the different cases are shown in Table I. Fig. 9 shows the air gap ratio against the ratio error and phase displacement for a primary current of 100 A. The effect of changing the length of the air gap in the core of the CT can be noted with the results obtained from the simulations presented in Table I and Fig 9.

From Table I can be seen that as the air gap ratio is increased, the error ratio and phase displacement increase as well. Hence, increasing the air gap will result in a reduction of the accuracy of the transformer that can be seen in the difference of amplitude and phase between the primary and

secondary current. If the air gap ratio is smaller, then the accuracy of the AGCT will improve.

TABLE I. RATIO ERROR AND PHASE DISPLACEMENT

Primary current (A)	Air gap ratio (%)	Ratio error (%)	Phase displacement (Centiradians)
100	0	0	0.00
	0.001	-4.99	14.20
	0.002	-12.23	29.19
	0.003	-19.88	37.70
	0.004	-27.54	51.01
	0.005	-34.76	59.19
200	0	0.05	0.00
	0.001	-5	16.37
	0.002	-12.25	25.09
	0.003	-19.9	40.11
	0.004	-27.55	49.65
	0.005	-34.75	60.54

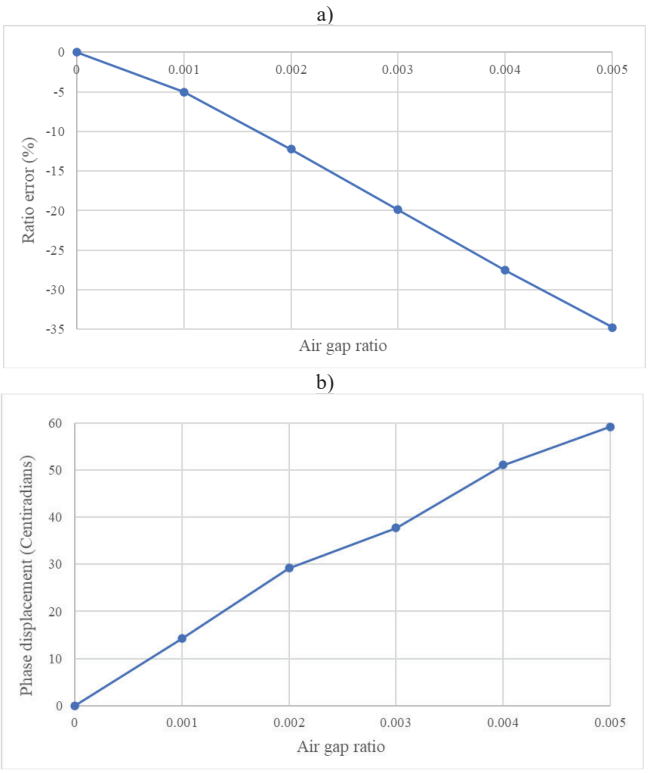

Fig. 9. Comparison between Air gap ratio and a)Ratio error b)Phase displacement with a primary current of 100 A.

From Fig. 9 it is observed that the behaviour of the air gap ratio with respect to the error ratio can be defined as a linear trend. Similar results for the error ratio were obtained for a current of 200 A. Analysing the results of the phase displacement, it is observed that this error is similar for both primary currents tested.

Finally, the results are evaluated according to the International Standard IEC 61869-2:2012 [19] for instrument transformers. This indicates that the accuracy classes for metering CTs are: 0.1, 0.2, 0.2S, 0.5, 0.5S, 1, 3 and 5. These classes are described by considering the limits of ratio error and phase displacement of the CT.

From measurements obtained it is found that only when the CT has no air gap can it be considered as a transformer with accuracy class of 0.1 for both primary current values tested. For a CT with an accuracy class of 0.1, the error ratio allowed is ±0.1% at 100% of the rated current and the phase displacement allowed is ±0.15 centiradians.

In the other cases where the air gap ratio is different from 0, the AGCT can only be considered to have an accuracy class of 5 when the air gap ratio is 0.001. According to the standard, the accuracy class 0.5 admits an error ratio of ±0.5% at 100% of the rated current and there are not specified limits for phase displacement in this class [19].

V. CONCLUSIONS

Current studies are focused on the development of a potential solution for the problem of DC injected into the grid and the challenges that Current Transformers for metering purposes may face. Previous research has concentrated on the solution through active devices such as filters or current compensation. The proposed solution consists of using an Air-gapped Current Transformer to face this issue. The advantages of introducing an air gap into the core of the CT are clear. Remanent flux will be drastically reduced, which will provide the CT with a better tolerance to DC injected into the network from modern equipment sources and devices.

Furthermore, most research about AGCTs focuses on their behaviour when they are used for protection purposes. Hence, the adoption of AGCTs for measuring purposes provides a different methodology to deal with the new challenges brought by smart grids.

The modelling and simulation of the AGCT is an effective way to observe the effects due to the change of different parameters of the system. An important point addressed in the paper is the loss of accuracy that the increase of the air gap has on the output of the transformer. The results obtained allow the designer to predict the behaviour of an AGCT taking into consideration the characteristics of the material, the air gap length, the length of the magnetic core, inductance load, resistance load, primary current, turns ratio and the cross-sectional area of the core.

Finally, the accuracy of the different cases of AGCTs has been evaluated according to the standard IEC. According to the results, it can be seen the increase in ratio error and phase displacement when the air gap ratio is increased. Results have shown that the AGCT accomplishes an accuracy of 0.1 when there is no air gap in the core and it has accuracy of 5 when the air gap ratio is 0.001. If the air gap ratio is increased, the AGCT does not accomplish the accuracy requirements for this standard. Accuracy of CTs is particularly important because these devices are used for metering and revenue purposes.

REFERENCES

[1] Lesniewska, E., Influence of the Selection of the Core Shape and Winding Arrangement on the Accuracy of Current Transformers with Through-Going Primary Cable. Energies, 2021. 14(7): p. 1932.

[2] Shi, Y., B. Liu, and S. Duan, Eliminating DC Current Injection in Current-Transformer-Sensed STATCOMs. IEEE Transactions on Power Electronics, 2013. 28(8): p. 3760-3767.

[3] Ripka, P., K. Draxler, and R. Styblikova. DC-compensated current transformer. in 2014 IEEE International Instrumentation and Measurement Technology Conference (I2MTC) Proceedings. 2014.

[4] Bachinger, F., et al., Direct current in transformers: effects and compensation. e & i Elektrotechnik und Informationstechnik, 2013.

[5] Conner, E.E., R.G. Greb, and E.C. Wentz, Control of Residual Flux in Current Transformers. IEEE Transactions on Power Apparatus and Systems, 1973. PAS-92(4): p. 1226-1233.

[6] Y. C, K., et al. Compensation of an Air-Gapped Current Transformer Considering the Hysteresis Characteristics of the Core. in 2008 IET 9th International Conference on Developments in Power System Protection (DPSP 2008). 2008.

[7] Yahyavi, M., F. Brojeni, and M. Vaziri. Basic Theory and Practical Considerations in a Current Transformer. in 2007 IEEE Power Engineering Society General Meeting. 2007.

[8] Fehr, R.E., Industrial Power Distribution. 2 ed. 2015, Nashville, TN: John Wiley & Sons.

[9] Hargrave, A., M.J. Thompson, and B. Heilman. Beyond the knee point: A practical guide to CT saturation. in 2018 71st Annual Conference for Protective Relay Engineers (CPRE). 2018.

[10] Wu, Y.H., X.Z. Dong, and S. Mirsaeidi, Modeling and simulation of air-gapped current transformer based on Preisach Theory. Protection and Control of Modern Power Systems, 2017. 2(1): p. 11.

[11] Gapped core current transformer characteristics and performance. IEEE Transactions on Power Delivery, 1990. 5(4): p. 1732-1740.

[12] Jiles, D.C. and D.L. Atherton, Theory of ferromagnetic hysteresis. Journal of Magnetism and Magnetic Materials, 1986. 61(1): p. 48-60.

[13] Del Moral Hernandez, E., C. S. Muranaka, and J.R. Cardoso, Identification of the Jiles–Atherton model parameters using random and deterministic searches. Physica B: Condensed Matter, 2000. 275(1): p. 212-215.

[14] Jiles, D.C. and D.L. Atherton, Theory of ferromagnetic hysteresis (invited). Journal of Applied Physics, 1984. 55: p. 2115.

[15] Kanokbannakorn, W. and T. Penthong. Improvement of a Current Transformer Model based on the Jiles-Atherton Theory. in 2019 IEEE PES GTD Grand International Conference and Exposition Asia (GTD Asia). 2019.

[16] Muthumuni, D., et al. Simulation model of an air gapped current transformer. in 2001 IEEE Power Engineering Society Winter Meeting. Conference Proceedings (Cat. No.01CH37194). 2001.

[17] Hergli, K., H. Marouani, and M. Zidi, Numerical determination of Jiles-Atherton hysteresis parameters: Magnetic behavior under mechanical deformation. Physica B: Condensed Matter, 2018. 549: p. 74-81.

[18] Cogent. Typical data for SURA®. M330-35A. 2009; Available from: https://www.tatasteeleurope.com/.

[19] IEC 61869-2:2012, in Instrument transformers - Part 2: Additional requirements for current transformers. 2012, International Electrotechnical Commission.